Flow, Turbulence and Combustion
https://doi.org/10.1007/s10494-023-00501-7

RESEARCH

Stochastic Modeling of Partially Stirred Reactor (PaSR) for the Investigation of the Turbulence-Chemistry Interaction for the Ammonia-Air Combustion

Chunkan Yu[1] · Liming Cai[2] · Jyh-Yuan Chen[3]

Received: 1 September 2023 / Accepted: 6 October 2023

Abstract
The Partially Stirred Reactor (PaSR) model is carried out for the ammonia-air combustion system by means of stochastic modeling, namely by solving the transport equation for the joint Probability Density Function (PDF). The turbulent mixing is accounted for by the Linear Mean-Square Estimation (LMSE) mixing model. Notwithstanding the simplified nature of the PaSR modeling, the transported-PDF method enables capturing the effect of mixing frequency on the combustion system, especially the NOx emission. Since the chemical source term is in a closed form in the transported-PDF method, it allows us to apply different chemical mechanisms to explore, whether the set of elementary reactions that are identified as important for the prediction of NOx in the PaSR model is sensitive to the choice of chemical mechanisms. Furthermore, the effect of the residence time in the PaSR model has also been studied, and compared with those in the Perfectly Stirred Reactor (PSR) model (infinite large mixing frequency). Moreover, since the ammonia under oxygen enrichment shows some similar combustion behaviors in terms of e.g. laminar burning velocity as the ammonia under hydrogen enrichment, how large the difference of thermo-kinetic states (e.g. temperature and NOx emission) predicted by PaSR models and in laminar premixed flame configuration is also investigated. A further discussion focuses on the effect of thermal radiation, where the radiative heat loss roles in the prediction of NOx for the turbulent simulation is examined. By using the optically thin approximation model, it is shown that the thermal radiation exhibits little effect on the considered combustion systems within a typical turbulent time-scale.

Keywords Partially stirred reactor (PaSR) · Probability density function (PDF) · Turbulent combustion · Ammonia

✉ Chunkan Yu
chunkan.yu@kit.edu

[1] Institute of Technical Thermodynamics, Karlsruhe Institute of Technology, Engelbert-Arnold-Straße 4, Karlsruhe 76131, Baden-Württemberg, Germany

[2] School of Automotive Studies, Tongji University, Cao'an Road No.4800, Shanghai 201804, People's Republic of China

[3] Department of Mechanical Engineering, University of California, Berkeley, 6163 Etcheverry Hall, Berkeley, CA 94720-1740, USA

Published online: 30 October 2023

1 Introduction

Ammonia is a zero-carbon fuel and has been considered as the next possible source for power supply and energy storage (Valera-Medina et al. 2018, 2021). Many studies involving ammonia combustion systems have been carried out over the last decade. Among them are for example the development of ammonia chemical kinetics (Shrestha et al. 2021; Gotama et al. 2022; Nakamura et al. 2017; Dai et al. 2020), numerical and experimental determination of laminar burning velocity (Shrestha et al. 2021; Rocha et al. 2021; Wang et al. 2021), forced ignition processes (Lhuillier et al. 2020; Fernández-Tarrazo et al. 2023; Lesmana et al. 2022; Yu et al. 2023), extinction and flammability limit (Lee and Kwon 2011; Ichimura et al. 2019; Richter et al. 2023) and many others. Unlike the traditional hydrocarbon fuels, the ammonia mixture has some special combustion properties such as low flammability, low laminar burning velocity, high ignition energy requirement and so on Valera-Medina et al. (2018, 2021). Furthermore, the ammonia system suffers from high nitrogen oxides (NOx) emissions in combustion, and the NOx emission is closely correlated with other combustion properties such as flame stability which is important for real-life applications. For example, under lean conditions, NOx emissions were prohibitive while stability was restricted to a very narrow equivalence ratio range. As shown in Valera-Medina et al. (2019); Mashruk et al. (2022); Rocha et al. (2019), ammonia-hydrogen-air combustion system close to lean conditions lead to prohibitive NOx emissions while stability was compromised because of a very narrow equivalence ratio range, and rich conditions would be more suitable for practical applications.

Moreover, the investigation of the turbulence effect on the ammonia combustion system is more practice-oriented, and the increasing number of literature focuses on the turbulent ammonia flame. For example, the effect of Karlovitz number on the turbulent premixed flame structure and turbulent burning velocity has been reported in Fan et al. (2022). In Abdelwahid et al. (2023); Chi et al. (2023); Tian et al. (2023) the effect of the molecular transport model on the flame structure and species prediction has been intensively studied, showing that the differential diffusion including thermal diffusion (Soret effect) has a large impact on the NO production and turbulent flame speed. However, DNS or LES further complicates the study on the turbulence-chemistry interaction since one must use detailed molecular transport model which increases the computational cost or the averaged reaction rate must be accurately modeled/solved or the CFD grid must be fine enough to resolve the flame structure. Various physical variables could have an impact on the chemical kinetics, which makes the investigation more complicated.

In order to explore the turbulence-chemistry interaction for ammonia combustion systems, a stochastic modeling for the Partially Stirred Reactor (PaSR) model developed by Correa (1993) and Chen (1997) is used, a PDF-method-based models where the temperature and composition concentrations are described by a joint PDF. While the conventional Perfectly Stirred Reactor (PSR) model considers infinite fast mixing process and can provide valuable insights into the chemical kinetics, the PaSR model has the advantage that it allows to investigate the interaction between chemistry and finite-rate mixing and subsequently provides useful information about the effect of mixing processes on the chemical kinetics (Correa 1993; Cannon et al. 1998). Moreover, since the Monte-Carlo method has been used for the numerical simulation of PaSR model, the chemistry can be solved in an exact manner without any modeling.

The objective of this work will focus on several interesting questions, that provide a better understanding of the ammonia combustion system under the interaction with mixing processes:

- How large is the impact of mixing frequency on the ammonia system? Whether the influence of mixing frequency is similar to those on the conventional hydrocarbon fuels (Cannon et al. 1998; Correa 1993). In addition, to the author's knowledge, there is still limited investigation on the statistical properties of the ammonia system. How the statistics change with mixing frequency is a very important question. The understanding of the statistics is especially important for those who want to use the presumed PDF method in the turbulent simulation (Pope 1985; Borghi 1988; Bray et al. 1989).
- How large is the impact of residence time on the ammonia system, especially on the NOx emission. Whether the influence of residence time in the PaSR model is the same as the one in the conventional PSR model. Moreover, it is of great interest to know which elementary reactions are important for the NOx emission, and whether these important reactions remain unchanged for different residence times. Such information helps us to better understand chemical kinetics and provides useful information for the development of chemical mechanisms.
- Since there are various chemical mechanisms developed for ammonia systems that have been validated against common combustion properties such as ignition delay times and laminar burning velocities, whether the difference on the predicted NOx emission under the consideration of finite-rate mixing process in the PaSR models behaves similar as the difference predicted by the PSR model. If the difference in the NOx emission is observed, whether the important elementary reactions for the prediction of NOx emission are the same even for different chemical mechanisms.
- Whether the statistics (or the PDFs) of thermo-kinetic quantities (e.g. temperature, species concentration) are similar for different chemical mechanisms?

Besides the physical variables (mixing frequency and residence time) and chemical kinetic models, thermal radiation has been proven to have a large impact on the structure of turbulence flames. As shown in various works such as Dos Santos et al. (2016); Xu et al. (2021); Giordano and Lentini (2001); Poitou et al. (2012); Cao et al. (2007), while the thermal radiation causes only slightly decrease of mean temperature for the turbulent flames (around 20 - 50 K) and almost no differences for major species, the prediction of minor species or pollutants (e.g. NOx and soot) can be largely influenced by considering the radiative heat loss. Although the turbulence-radiation interaction has been intensively investigated for various hydrocarbon systems (Cao et al. 2007; Ilbas 2005; Giordano and Lentini 2001), there are limited studies about this topic for the ammonia combustion system. To the author's knowledge, only Nakamura et.al. in Nakamura and Shindo (2019) investigated intensively the thermal radiation effect on the ammonia-hydrogen-air system based on the simple optical thin approximation model (OTM) for unstrained laminar premixed flame configurations, confirming that the radiative heat loss has a strong effect on the laminar flame speed and the NOx emission in the high temperature regimes. However, the turbulence-radiation interaction for the ammonia-air system is still not investigated. Therefore, the novelty of this work regarding thermal radiation would be focused on understanding the impact of thermal radiation on the flame quantities?

2 Stochastic Modeling and Simulation of the Partially Stirred Reactor (PaSR)

2.1 Stochastic Modeling

The considered PaSR model is schematically illustrated in Fig. 1. The computational cell is split into three steps: one describing a through-flow process, one where reactions take place, and another characterized by only mixing. The final species concentration of the cell is determined from the mass exchange, characterizing the turbulence intensity.

Suppose we have the thermo-kinetic state vector $\vec{\phi}$ including scalars specific enthalpy h (in unit J/kg), pressure p (in unit Pa) and mass fractions of i-th species Y_i:

$$\vec{\phi} = \left(h, p, Y_1, Y_2, \cdots, Y_i, \cdots, Y_{n_s-1}, Y_{n_s}\right)^{\mathrm{T}}, \tag{1}$$

where n_s is the number of species involved in the chemical reactions. According to the Chen (1997), the stochastic modeling of the PaSR can be achieved by solving the transport equation for the joint Probability Density Function (PDF). The PDF applied in the PaSR modeling is the single-point joint scalar PDF $f_{\vec{\phi}}(\vec{\psi}, t)$, and the resulting joint PDF equation for the PaSR is Chen (1997)

$$\begin{aligned}\frac{\partial \widetilde{f}_{\vec{\phi}}(\vec{\psi}, t)}{\partial t} = &+ \frac{1}{\tau_{\mathrm{res}}}\left\{\widetilde{f}_{\vec{\phi},\mathrm{inlet}}(\vec{\psi}, t) - \widetilde{f}_{\vec{\phi}}(\vec{\psi}, t)\right\} - \sum_{\alpha=1}^{n_s+2} \frac{\partial}{\partial \psi_\alpha}\left\{\mathcal{R}_\alpha(\vec{\psi}) \cdot \widetilde{f}_{\vec{\phi}}(\vec{\psi}, t)\right\} \\ &- \sum_{\alpha=1,\beta=1}^{n_s+2} \frac{\partial^2}{\partial \psi_\alpha \psi_\beta}\left\{\langle \varepsilon_{\alpha\beta} | \vec{\phi} = \vec{\psi}\rangle \widetilde{f}_{\vec{\phi}}(\vec{\psi}, t)\right\},\end{aligned} \tag{2}$$

where $\mathcal{R}_\alpha$ is the source term of $\alpha-$th species in $\vec{\phi}$, and $\varepsilon_{\alpha\beta}$ the cross-scalar dissipation rate. In this equation, there exists three important time-scales: one is the residence time τ_{res}, second one the mixing time-scale τ_{mix} in the term of cross-scalar dissipation rate, and the third one the chemical time-scale τ_{reac} determined by the eigenvalue of the Jacobian matrix of the chemical source term (Maas and Pope 1992).

The first two terms on the right hand side of Eq. 2 represent the effect of the through-flow and the chemical reaction processes on the joint PDF. Both terms can be solved in a

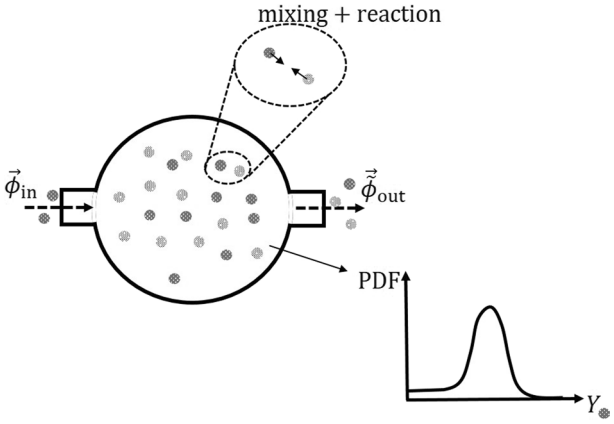

Fig. 1 Schematic illustration of PaSR model

detailed way, and the simulation can be performed with detailed chemical kinetics without additional modeling and computing limitations. The third term on the right hand side of Eq. 2 stands for the effect of the micro-scale mixing process on the joint PDF, which needs to be modeled.

The transported PDF equation can be computed efficiently by using the Monte-Carlo particle method (Pope 1985), where the PDF $f_{\vec{\phi}}(\vec{\psi}, t)$ is represented by the N_p-number of notional particles. Each notional particle k includes the information of specific enthalpy, pressure and mass fractions of $i-$th species in the thermo-kinetic state vector $\vec{\phi}^{(k)} = (h^{(k)}, p^{(k)}, Y_i^{(k)})^{\mathrm{T}}$. Based on the $\vec{\phi}^{(k)}$, the ensemble-averaged values of thermo-kinetic state can be determined as

$$\langle \vec{\phi} \rangle = \frac{1}{N_p} \sum_{k=1}^{N_p} \vec{\phi}^{(k)}, \tag{3}$$

and the root mean square (r.m.s.) of the fluctuation, $\vec{\phi}' = \vec{\phi}^{(k)} - \langle \vec{\phi} \rangle$, can be calculated as

$$\text{r.m.s.}(\vec{\phi}') = \sqrt{\langle \vec{\phi}'^2 \rangle} = \sqrt{\frac{1}{N_p} \sum_{k=1}^{N_p} \left(\vec{\phi}^{(k)} - \langle \vec{\phi} \rangle \right)^2}. \tag{4}$$

The evolution of the thermo-kinetic state of particle k due to reaction and molecular mixing process can be expressed in the ODE system:

$$\frac{\mathrm{d}\vec{\phi}^{(k)}}{\mathrm{d}t} = \mathcal{M}\left(\vec{\phi}^{(1)}, \vec{\phi}^{(2)}, \cdots, \vec{\phi}^{(n_p)} \right) + \mathcal{R}\left(\vec{\phi}^{(k)} \right), \tag{5}$$

where $\mathcal{M}$ stands for the mathematical description of the molecular mixing process.

For an isobaric combustion system, which is also the case studied in the present work, the thermo-kinetic source term reads

$$\mathcal{R}\left(\vec{\phi}^{(k)} \right) = \left(\dot{q}_{\mathrm{rad}}^{(k)}, 0, \frac{\dot{\omega}_1^{(k)} W_1}{\rho}, \cdots, \frac{\dot{\omega}_i^{(k)} W_i}{\rho}, \cdots, \frac{\dot{\omega}_1^{(n_s)} W_{n_s}}{\rho} \right)^{\mathrm{T}}, \tag{6}$$

where $\dot{\omega}_i$ and W_i are the net production rate and molar mass of species i, and ρ is the density of the gas mixture. The symbol $\dot{q}_{\mathrm{rad}}^{(k)}$ stands for the radiative heat loss rate per unit mass (J/(kg·s)):

$$\dot{q}_{\mathrm{rad}}^{(k)} \begin{cases} = 0 & \text{adiabatic system,} \\ < 0 & \text{existence of radiation} \end{cases} \tag{7}$$

The term $\mathcal{M}$ is a crucial issue in the simulation of transported PDF equation, since its modeling can largely affect the numerical prediction (Chang and Chen 1996; Cao et al. 2007). According to Pope (1985), the term of cross-scalar dissipation rate in Eq. 2, in which scalar diffusion, conditional upon the scalar value, must be modeled in the way, such that the decay of the scalar fluctuation should admit $\mathrm{d}\langle \vec{\phi}'^2 \rangle / \mathrm{d}t = -2 C_\phi \omega_{\mathrm{mix}} \langle \vec{\phi}'^2 \rangle$, where C_ϕ is the mixing model parameter and ω_{mix} the mixing frequency. An explicit approximation of this term is the Linear Mean-Square Estimation (LMSE) (Dopazo and O'Brien 1974), a mixing model is one of the most simple but commonly used mixing models, which can give the correct decay of scalar fluctuation. For this model, the evolution of the thermo-kinetic states of the particle k is expressed via an ordinary differential equation

$$\frac{\mathrm{d}\vec{\phi}^{(k)}}{\mathrm{d}t} = -\frac{1}{2} C_\phi \omega_{\mathrm{mix}} \cdot \left(\vec{\phi}^{(k)} - \langle \vec{\phi} \rangle \right), \tag{8}$$

in which $\langle \vec{\phi} \rangle$ the mean value of the thermo-kinetic states of N_p particles.

Note that although the LMSE is simple and gives reasonable prediction for various cases (Cao et al. 2007; Raman and Pitsch 2007), the principle deficiency of LMSE model is the fact that the shape of the scalar PDF remains unchanged due to the absence of mean scalar gradient and thus never relaxes to Gaussian distribution (Celis and Silva 2015; Fox 2003). Therefore, many other advanced mixing models have been developed. Among them are e.g. the Euclidean Minimum Spanning Trees (EMST) model (Subramaniam and Pope 1998), the Multiple Mapping Conditioning (MMC) model (Cleary and Klimenko 2009) and the shadow-position conditioning mixing model (SPMM) (Pope 2013).

2.2 Numerical Implementation

The numerical simulation has been performed by using the self-written *PaSR4Comb* package, a MatLab-based code coupled with Cantera (Goodwin et al. 2022) for the simulation of PaSR for combustion system, which is also available for download in Github via (Yu 2023). The numerical simulation follows the procedure described in Chen (1997), namely a fractional step scheme with a time step Δt is used to determine the PDF equation for the PaSR (c.f. Eq. 2), and particles are assumed to have the same weight. For each time step, the following three steps are performed:

(i) Through-flow: For this step, N_{replaced} notional particles are randomly selected from the whole stochastic ensemble, and replaced by the notional particles with thermo-kinetic states of incoming mixture properties $\vec{\phi}_{\mathrm{inlet}}$. The N_{replaced} is calculated via

$$N_{\mathrm{replaced}} = N_p \cdot \frac{\Delta t}{\tau_{\mathrm{res}}}. \tag{9}$$

Note that if N_{replaced} is less than one, the N_{replaced} is saved and accumulated until it reaches one and then replaces the particle accordingly.

(ii) Molecular mixing process: The mixing process will be performed for the time step Δt. For the mixing model, the model parameter C_ϕ must be given *a-priori*. In the present work, only the LMSE mixing model will be used. For the LMSE model, the thermo-kinetic state after mixing can be calculated in a deterministic way and the analytical solution reads:

$$\vec{\phi}^{(k)}_{\mathrm{new}} = \langle \vec{\phi} \rangle + \left(\vec{\phi}^{(k)} - \langle \vec{\phi} \rangle \right) \cdot \exp\left(-\frac{1}{2} C_\phi \omega_{\mathrm{mix}} \Delta t \right) \tag{10}$$

(iii) Chemical reaction process: During this reaction process step, the thermo-kinetic states of the notional particles are evolved due to chemical reaction with the time step Δt following the ordinary differential equation (ODE)

$$\frac{\mathrm{d}\vec{\phi}^{(k)}}{\mathrm{d}t} = \mathcal{R}\left(\vec{\phi}^{(k)} \right). \tag{11}$$

The initial condition for this chemical reaction process is the thermo-kinetic states of the notional particles after the mixing process. In the code, the chemical source

term is evaluated through the Cantera (Goodwin et al. 2022), and the ODE system is computed by using in-built *ode15s*, a variable-step variable-order (VSVO) solver in Matlab for the numerical integration of stiffness ODE (Shampine and Reichelt 1997).

For the starting point, all particles inside the PaSR at $t = 0$ have the thermo-kinetic states under equilibrium conditions.

2.3 Validation of the *PaSR4Comb* Package

The *PaSR4Comb* (Yu 2023) has been validated against various existing simulation results in different works such as Cannon et al. (1998); Correa (1993); Chen (1997). Before continuing our discussion on the ammonia-air combustion system, we shortly show in this section the validation of the implemented algorithm applied in *PaSR4Comb* package.

Figure 2 shows the comparison of ensemble-averaged temperature $\langle T \rangle$ and NO emission $\langle \mathrm{NO} \rangle$ versus mixing frequencies from Cannon et al. (1998) (in lines) and from *PasR4Comb* code (in symbols). The GRI 2.11 mechanism is used and the CH_4-air mixture with three different fuel/air equivalent ratios is considered. The results from *PasR4Comb* code are based on exact identical model and numerical parameters from Cannon et al. (1998). We notice that there are almost no observable differences between both results, showing the correctness of *PaSR4Comb* code.

3 Combustible Gas System

In the present work, we focus on the stoichiometric 70%NH_3-30%H_2-air combustion system. This 70%-30% (vol) ammonia-hydrogen blend has been investigated in many works for different purposes such as spark ignition engines and gas turbines (Chiong et al. 2021; Mashruk et al. 2022; Xiao et al. 2017; Valera-Medina et al. 2019), showing that 30% (vol) hydrogen in an ammonia mixture could produce high power as methane and provides wide operational range with considerably stable combustion property (Mashruk et al. 2022; Chiong et al. 2021). Figure 3 shows the tendency of adiabatic temperature and NOx concentration against the residence time τ_{res} for a PSR model, which corresponds to

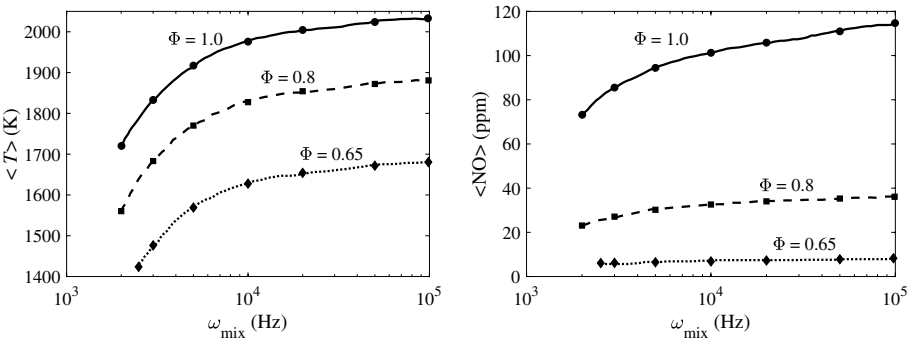

Fig. 2 Dependence of ensemble-averaged temperature $\langle T \rangle$ and NO emission $\langle \mathrm{NO} \rangle$ on mixing frequencies ω_{mix}. Mixture: methane-air. Mechanism: GRI 2.11. Lines: simulation results from Cannon et al. (1998). Symbols: simulation results using *PaSR4Comb* code

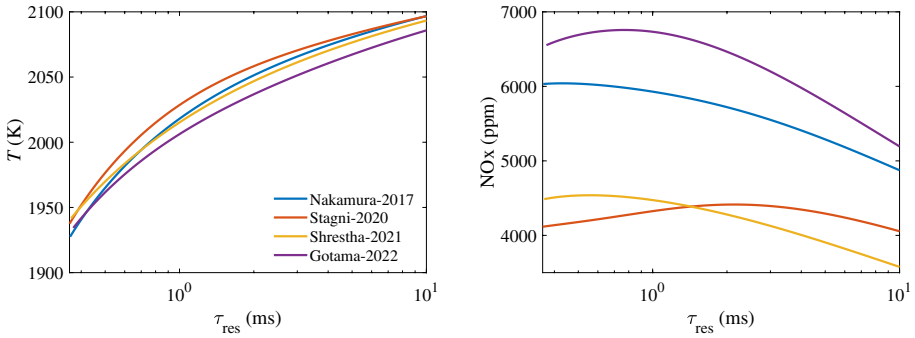

Fig. 3 Tendency of adiabatic temperature and NOx concentration against the residence time τ_{res} for a PSR model. Blue: Nakamura-2017 (Nakamura et al. 2017); Red: Stagni-2020 (Stagni et al. 2020); Yellow: Shrestha-2021 (Shrestha et al. 2021); Purple: Gotama-2022 (Gotama et al. 2022)

the PaSR model with $\omega_{mix} \to \infty$. Also, four different chemical mechanisms developed for the ammonia-hydrogen-air system are applied. Here, the PSR calculation is consistent with the model proposed in Glarborg et al. (1986).

As expected the adiabatic temperature at a steady state in PSR drops as residence time becomes shorter due to shorter available reaction time, which is consistent with many works such as Hottel et al. (1958); Lu and Law (2005); Rutar et al. (1998); Turns (1996). The behavior of NOx (including NO and NO_2), on the other hand, is more complicated, with maxima exhibited at a certain residence time (more explanation in Sec. 4.3). Furthermore, we notice that the temperature profiles predicted by different mechanisms are similar, while the predicted NOx concentrations can be significantly different. However, the tendency is the same for all tested mechanisms, namely the NOx concentration has a peak at a certain residence time.

It is also observed that the extinction residence time (very left point), below which no burning solution can be obtained, is almost similar even with different chemical mechanisms. This is because all four mechanisms have been well validated against the experimental measurement of ignition delay time.

In the following, we select the Shrestha-2021 mechanism for our further discussion about the influence of mixing frequency and residence time because of the following two reasons:

- It has been validated for different purposes such as ignition delay times and laminar flame speeds intensively against experiment measurements (Shrestha et al. 2021).
- This mechanism was also proven to give an accurate prediction for the oxygen-enriched ammonia-air system (Shrestha et al. 2021) in terms of laminar flame speed. Later, the effect of hydrogen addition and oxygen addition in the ammonia-air mixture for the PaSR model will be examined.

However, the influence of both mixing frequency and residence time on the NOx concentration predicted by the other three detailed mechanisms will also be discussed shortly, showing that the obtained results and observation are not affected by the chemical mechanisms.

Moreover, if not specified, the adiabatic system is considered, which means a zero radiative heat loss in the equation ($q_{\mathrm{rad}} = 0$ in Eq. 7). However, the effect of the radiation on the predicted ensemble-averaged quantities, especially on the NOx emission which is very sensitive to the temperature, will be still investigated. As reported in Nakamura and Shindo (2019); Zheng et al. (2023), the thermal radiation can change the flame structure, species concentrations and minimal ignition energy for the ammonia-hydrogen-air combustion system. The radiation model used in the present work follows the one from Nakamura and Shindo (2019), namely the optically thin approximation model (OTM), where the volumetric radiative heat loss $\dot{Q}_{\mathrm{rad}}$ in J/(m^3·s) is given as:

$$\dot{Q}_{\mathrm{rad}} = \rho \cdot \dot{q}_{\mathrm{rad}} = 4 \cdot k \cdot \sigma \cdot \left(T^4 - T_{\mathrm{b}}^4\right) \tag{12}$$

here $\sigma = 5.669 \cdot 10^{-8}$W/(m^2·K^4) is the Stefan-Boltzmann constant. T is the local temperature and T_{b} is the background temperature ($T_{\mathrm{b}} = T_{\mathrm{ub}}$). k is the total Planck mean absorption coefficient, and determined as $k = \sum p_i a_{p,i}$, where p_i is the partial pressure of radiating species i in and $a_{p,i}$ the Planck mean absorption coefficient of radiation species i. Following the model in Nakamura and Shindo (2019), the H_2O, NO, N_2O and NH_3 are the four most important radiating species in the ammonia-hydrogen-air system, and their $a_{p,i}$ values can be found in Nakamura and Shindo (2019). Figure 4 shows the dependence of a_p on the temperature range $T \in [300\ \mathrm{K}, 2500\ \mathrm{K}]$ for all involved four radiating species.

4 Results: Effect of PaSR Model Parameters

In this section, the effect of PaSR model parameters, the mixing frequency ω_{mix} and the residence time τ_{res}, on the thermo-kinetic quantities of the combustion system at the stochastic steady state will be discussed. Note that throughout the whole work, the mixing frequency ω_{mix} is assumed to be equal for all thermo-kinetic states.

We consider the configuration that has only one stream describing the stoichiometric premixed mixture (70%NH_3–30%H_2-air) flows into the reactor with temperature $T_{\mathrm{in}} = 300$ K. The pressure of the whole system is controlled unchanged with $p = 1$ bar.

The LMSE mixing model with the standard mixing model parameter $C_\phi = 2.0$ will be used. Moreover, the marching time step $\Delta t = 1 \times 10^{-6}$ s and 800 notional particles ($N_p = 800$) are applied, and a further decrease of Δt and a further increase of N_p do not alter the ensemble-averaged thermo-kinetic quantities at stochastic steady state.

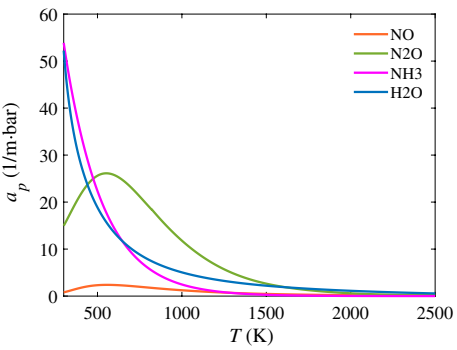

Fig. 4 Planck mean absorption coefficients of radiation species in ammonia-hydrogen-system against temperature ranges

4.1 Convergence to Stochastic Steady State

Figure 5 shows the typical convergence of the ensemble-averaged temperature $\langle T \rangle$, NOx emission $\langle \mathrm{NOx} \rangle$ and mole fractions of NH_3 $\langle x_{\mathrm{NH3}} \rangle$ and HNO $\langle x_{\mathrm{HNO}} \rangle$ for different mixing frequencies ω_{mix}. The dependence of the ensemble-averaged values of different quantities at the stochastic steady-state on the mixing time will be discussed in the next section. The main observation here is that the proposed algorithm described above according to Chen (1997) converges to a stochastic steady state for every case as well as for the ammonia-hydrogen combustion system. Note that the x-axis describes the non-dimensional time $\omega_{\mathrm{mix}} \cdot t$. According to Chen (1997), for a given residence time, the time to reach the stochastic steady state could be correlated inversely to the mixing frequency by using the LMSE model. Therefore, we observe that for different mixing frequencies, the steady states reach about the same $\omega_{\mathrm{mix}} \cdot t$ point if they start from the same initial conditions.

4.2 Effect of Mixing Frequency

4.2.1 Tendency Against the Mixing Frequency

As previously shown in Cannon et al. (1998); Correa (1993) for methane-air combustion system, the PaSR results tend to their PSR results in the limit of infinite large mixing

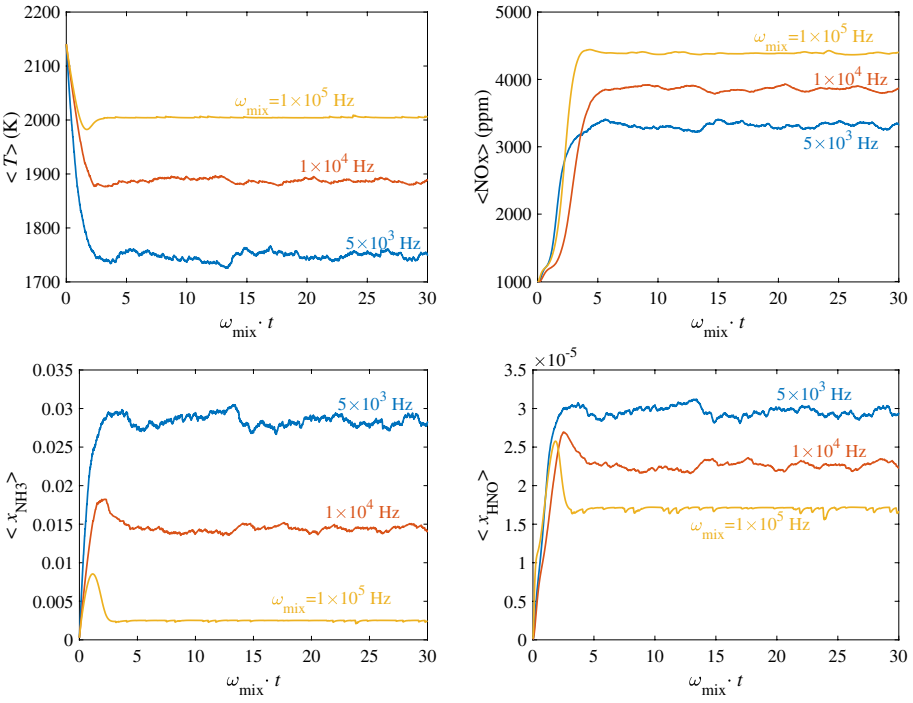

Fig. 5 Convergence of the ensemble-averaged temperature $\langle T \rangle$, NOx emission $\langle \mathrm{NOx} \rangle$ and mole fractions of NH_3 $\langle x_{\mathrm{NH3}} \rangle$ and HNO $\langle x_{\mathrm{HNO}} \rangle$ for different mixing frequencies ω_{mix}. $\tau_{\mathrm{res}} = 1$ ms. Mixture: 70%NH_3+30%H_2 +air. Adiabatic system

frequency ($\omega_{\mathrm{mix}} \to \infty$) and one obtains extinction results for small mixing frequency. Furthermore, the fluctuation of thermo-kinetic states decreases with increasing turbulent frequency, and it approaches zero for $\omega_{\mathrm{mix}} \to \infty$. These observations have also been observed for the considered ammonia-hydrogen-air system, which is clearly shown in Fig. 6.

It shows the influence of mixing frequencies ω_{mix} on the ensemble-averaged temperature $\langle T \rangle$ and NOx emission $\langle \mathrm{NOx} \rangle$ for the case with residence time $\tau_{\mathrm{res}} = 1$ ms. Note that although the discussion is based on one certain residence time, the conclusion is also valid for other residence times, which can be observed in Fig. 9 including different residence times till extinction limit. It should be mentioned at first that the curves end at the extinction mixing frequency $\omega^{\mathrm{E}}_{\mathrm{mix}}$ (the very left point), below which combustion system is quenched and no burning solution is obtained (all particles have the temperature same as the temperature of incoming cold particles). Furthermore, if the mixing frequency is infinitely large ($\omega_{\mathrm{mix}} \to \infty$), the results tend to the PSR limit.

A clear observation is that the thermo-kinetic quantities decrease monotonically with decreasing mixing frequency, which is consistent with those shown in Cannon et al. (1998); Correa (1993) for methane-air combustion system. With the decrease in mixing frequency, the mixing intensity between the incoming cold particles and hot particles inside the reactor decreases, leading to a lower temperature of cold particles after mixing and a longer time for ignition. Therefore the averaged values of thermo-kinetic quantities decrease due to increasing incomplete mixing (smaller mixing frequency). If the mixing frequency is below the extinction mixing frequency $\omega_{\mathrm{mix}} < \omega^{\mathrm{E}}_{\mathrm{mix}}$, the temperature of incoming cold particles increased after mixing is too low, so that the ignition temperature cannot be reached and these particles cannot be successfully ignited to support for further combustion.

Moreover, it is observed that the r.m.s.(T') and r.m.s.($\mathrm{NO}'_{\mathrm{x}}$) increase with decreasing mixing frequency. This is because the disparity between low-temperature and high-temperature particles becomes larger when the mixing frequency decreases. In other words, if the mixing frequency is larger, all particles are relaxed to or close to their mean values $\langle \phi \rangle$, so that all particles have the same or similar values after mixing, leading to smaller fluctuation and thus smaller corresponding r.m.s.. In the PSR limit case where $\omega_{\mathrm{mix}} \to \infty$, the corresponding r.m.s. values tend to vanish, since all the particles are perfectly mixed and have the same thermo-kinetic states.

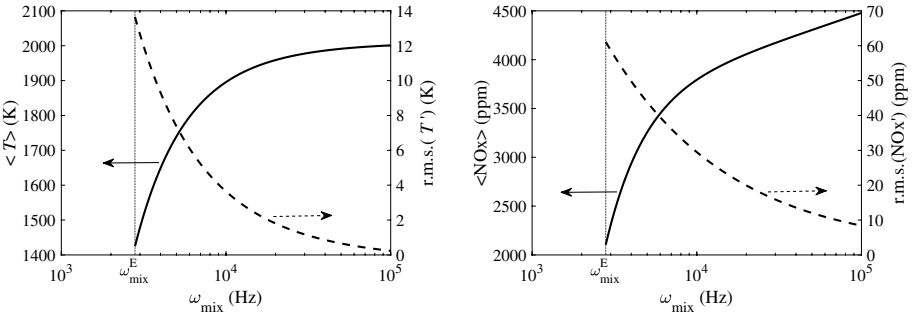

Fig. 6 Influence of mixing frequencies ω_{mix} on the ensemble-averaged temperature $\langle T \rangle$ and NOx emission $\langle \mathrm{NOx} \rangle$ (left y-axis) and their r.m.s. of the fluctuation (right y-axis). $\tau_{\mathrm{res}} = 1$ ms. Mixture: 70%$\mathrm{NH_3}$+30%$\mathrm{H_2}$ +air. Adiabatic system

4.2.2 Statistics of Thermo-Kinetic States

Since the mixing frequency has a significant impact on the ensemble-averaged values of thermo-kinetic states, it is worth checking the influence of the mixing frequency on the PDF of thermo-kinetic states from the notional particles. Figure 7 shows the PDFs of temperature and NOx at statistical steady state for different mixing frequencies for 1 ms residence time as an example. Since the LMSE is a deterministic mixing model in which all thermo-kinetic states of the particles are relaxed to their mean values, the predicted temperatures and NOx follow a single trajectory without scatter, which is also observed in Chang and Chen (1996).

It is noticed from Fig. 7 that for a large mixing frequency (red and yellow bars here), only one peak in the PDF of temperature and NOx is observed, corresponding to the decreasing r.m.s. of the fluctuations. As the mixing frequency becomes smaller (blue bars here), we observe one PDF peak at the high temperature and a noticeable PDF at the low

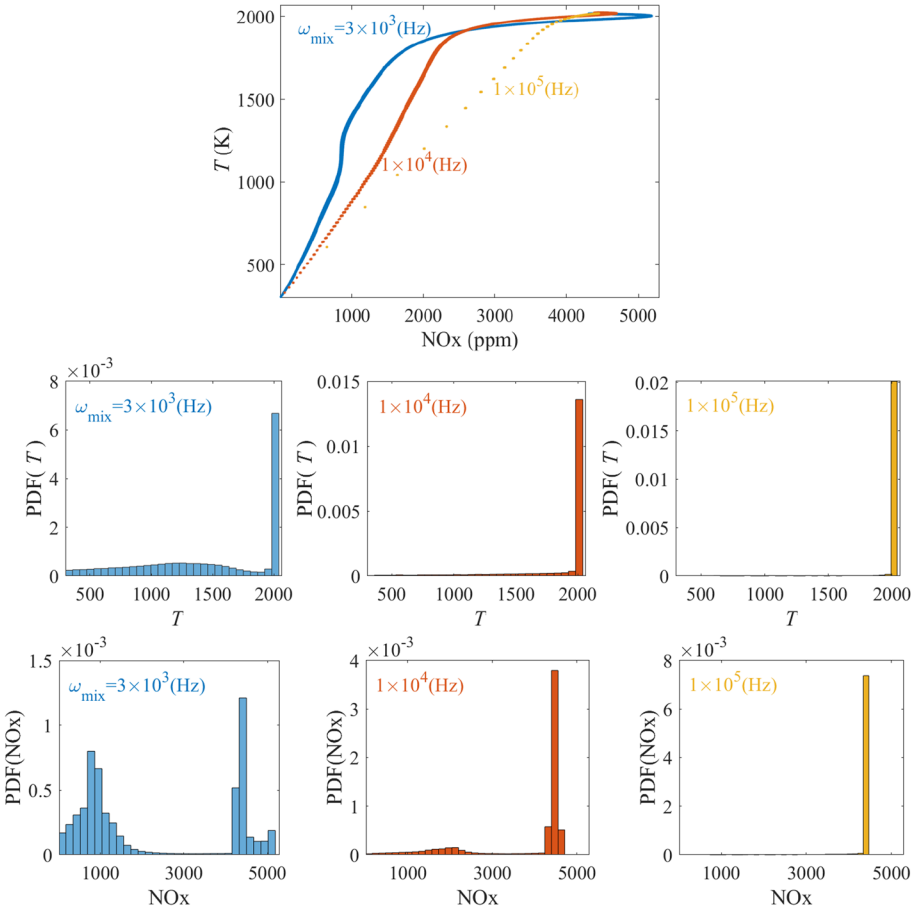

Fig. 7 Scatter plots and PDFs of temperature and NOx at statistical steady state. Residence time: τ_{res} = 1 ms. Mixture: 70%NH_3–30%H_2-air. Adiabatic system. Three different turbulent frequencies from Fig. 6 are selected

temperature. Furthermore, we observe two peaks in the PDF of NOx as well: one corresponds to the existence of cold particles with low values of NOx; the other to the existence of hot particles with high values of NOx. This information would be helpful for the statistical modeling of turbulent ammonia-hydrogen combustion systems based on the presumed PDF method, in which the shapes of the PDF must be presumed for the solution of transported-PDF method (Pope 1985; Borghi 1988; Bray et al. 1989). While the commonly used presumed β–PDF (Landenfeld et al. 2002; Mukhopadhyay et al. 2015; Salehi and Bushe 2010; Wang et al. 2016) can be reasonable for flows with larger mixing frequencies where only one PDF peak is observed, it can be inaccurate for the prediction of NOx for flows with smaller mixing frequencies because the β–function cannot combine a peak for burnt gases with an intermediate peak between the unburnt fresh gas and burnt gas (Poinsot and Veynante 2005) such as the PDF of NOx here.

4.2.3 Statistical Independence of Thermo-Kinetic Variables

In the simulation based on the presumed PDF method, the multivariate joint PDF must be presumed if multi-dimensional progress variables are used (Landenfeld et al. 2002; Wang et al. 2016). For example, the joint PDF for composition is $\mathrm{PDF}(\vec{\phi}) = \mathrm{PDF}(\phi_1, \phi_2, \cdots, \phi_j)$, the assumption of statistical independence is usually employed (Poinsot and Veynante 2005; Shrotriya et al. 2020; Landenfeld et al. 2002), leading to the joint PDF being equal to the product of the single PDFs as $\mathrm{PDF}(\vec{\phi}) = \mathrm{PDF}(\phi_1) \cdot \mathrm{PDF}(\phi_2) \cdot \cdots \cdot \mathrm{PDF}(\phi_j)$.

Although such statistical independence assumption is numerically simple to implement, it is shown that such assumption may give inaccurate prediction (Marchisio et al. 2001; Gerlinger 2003). Therefore, it is worth investigating the PDF based on two variables for the ammonia-hydrogen system, whether different thermo-kinetic variables are statistical independent.

In Fig. 8 the joint PDF of x_{NH2} and x_{NNH} (left figure) and the joint PDF of x_{N2} and x_{NNH} (right figure) are presented. These three species are selected because, according to Chen et al. (2021), a large amount of NH_2, dissociated from NH_3, will be consumed to NNH and further to major product N_2. From the figure we observe again that for large mixing frequency (here yellow bars), the peak of joint PDF occurs in the hot particles regime (marked with pink circles), indicating that most of the NH_2 is transferred to major product N_2 (Chen et al. 2021). However, if the mixing frequency is low (here blue bars), we observe a small PDF peak in the cold particles regime (marked with green circles),

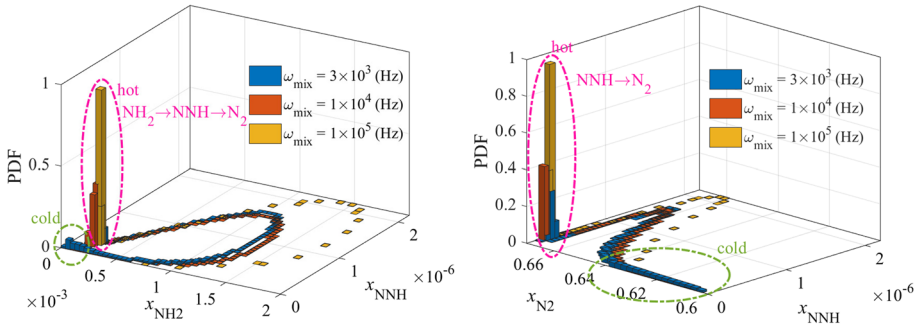

Fig. 8 Joint PDF of x_{NH2} and x_{NNH} (left figure) and joint PDF of x_{N2} and x_{NNH} (right figure) for different mixing frequencies ω_{mix}. $\tau_{\mathrm{res}} = 1$ ms. Mixture: 70%NH_3–30%H_2-air. Adiabatic system

indicating that in the statistical steady state a certain amount of produced NH_2 cannot be further transferred to NNH and N_2 due to low mixing intensity between cold particles and hot particles. This study tells us that for small mixing frequency, it may be inaccurate to simplify the joint PDF to a product of involved one-variable PDFs (here e.g. $\mathrm{PDF}(x_{\mathrm{NH2}}, x_{\mathrm{N2}}) \neq \mathrm{PDF}(x_{\mathrm{NH2}}) \cdot \mathrm{PDF}(x_{\mathrm{N2}})$), since these variables are strongly dependent on each other. In this case, the construction of presumed multi-dimensional PDF becomes much more difficult (Poinsot and Veynante 2005; Pope 1985; Lockwood and Naguib 1975).

4.3 Effect of Residence Time

In this part, the effect of residence time τ_{res} on the PaSR prediction will be discussed. Figure 9 shows the dependence of ensemble-averaged temperature $\langle T \rangle$ and NOx emission $\langle \mathrm{NOx} \rangle$ on the residence time for different mixing frequencies under the consideration of 70%NH_3–30%H_2-air adiabatic system. The PSR results are also presented as comparative model, corresponding to the PaSR with $\omega_{\mathrm{mix}} \to \infty$.

4.3.1 Tendency Against the Residence Time

It is clearly observed that all the PaSR results (with different ω_{mix}) are below the PSR results, and they end up with different extinction residence time τ_{res}^{E} (the very left point), below which no stable burning solution can be obtained. And for the smaller ω_{mix}, τ_{res}^{E} becomes longer. This is easy to understand because the disparity of the thermo-kinetic states of notional particles increases with decreasing ω_{mix}, therefore more particles are with lower temperatures compared to those under ω_{mix} and consequently need longer time to be ignited. Hence a longer residence time is required for cold particles to be ignited with sufficient long time at low ω_{mix}.

Furthermore, we observe here that for $\omega_{\mathrm{mix}} = 1 \times 10^5$ (Hz), the PaSR results and PSR results for both temperature and NOx emission shown here are almost overlap, with the difference only at short τ_{res} regime. This suggests that the PSR model can be used to describe the turbulence-chemistry-interaction for the combustion simulation, if the the thermo-kinetic states in the flow field tend to be mixed in a highly homogeneous manner, which is also discussed and investigated in Minamoto and Swaminathan (2015); Chen et al. (2017); De et al. (2011). On the other hand, with the decreasing residence time, the PaSR results

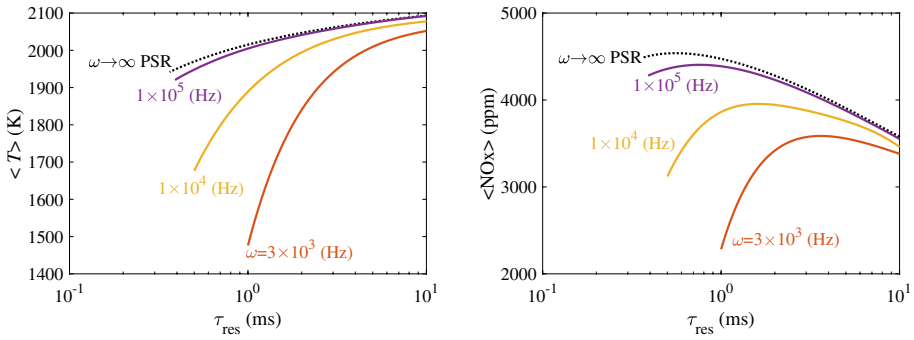

Fig. 9 Dependence of ensemble-averaged temperature $\langle T \rangle$ and NOx emission $\langle \mathrm{NOx} \rangle$ on the residence time for different mixing frequencies. Mixture: 70%NH_3–30%H_2-air. Adiabatic system

further depart from the PSR results, indicating that the PSR is not suitable for the turbulence-chemistry interaction if the mixing frequency is small.

While the temperature decreases monotonically with decreasing residence time, the NOx concentration shows non-monotonic behaviors against residence time, and a peak at a certain residence time for all cases. According to the reaction pathway analysis in Chen et al. (2021); Singh et al. (2022), under the hydrogen enrichment, NO is the primary component of NOx which is also several orders of magnitude higher than the NO_2. Furthermore, the NOx can be both produced from e.g. educt NH_3 and consumed to produce other species such as N_2O and N_2. Therefore, the level of NOx concentration results from the competition between the consumption time-scale and the production time-scale. For the PaSR model, at long residence time, the consumption time-scale for the NOx is sufficiently long, leading to a smaller amount in the stochastic steady state, because NOx can be further consumed. With decreasing residence time, the production time-scale for NOx is longer than its consumption time-scale, and NOx which is produced from NH_3 cannot be further consumed. Therefore, the NOx concentration concentration increases and reaches a peak at a certain residence time. If the residence time further decreases, the production time-scale of NOx is comparable short so that NOx cannot be produced from educt. In this way, the concentration of NOx decreases with decreasing residence time again, until the extinction residence time reaches and the combustion system quenches.

4.3.2 Statistics of NOx

In this part, it is interesting to see how the statistics in terms of PDF will be changed with residence time. Therefore, in Fig. 10 we show the PDFs of NOx at statistical steady state for two different residence times $\tau_{res} = 0.65$ ms and $\tau_{res} = 5$ ms. The selection of both residence times is based on the reason that the corresponding predicted $< NO_X >$ have almost the same values (c.f. Fig. 9), but they have totally different PDFs (c.f. Fig. 10).

For a long residence time (here $\tau_{res} = 5$ ms), the PDF with one peak is observed, showing that new incoming cold particles have enough time to be ignited after mixing and most of the particles have the same thermo-kinetic states. For this case, a commonly used β -function with suitable parameter choice is reasonable to describe the PDF of the NOx with one peak.

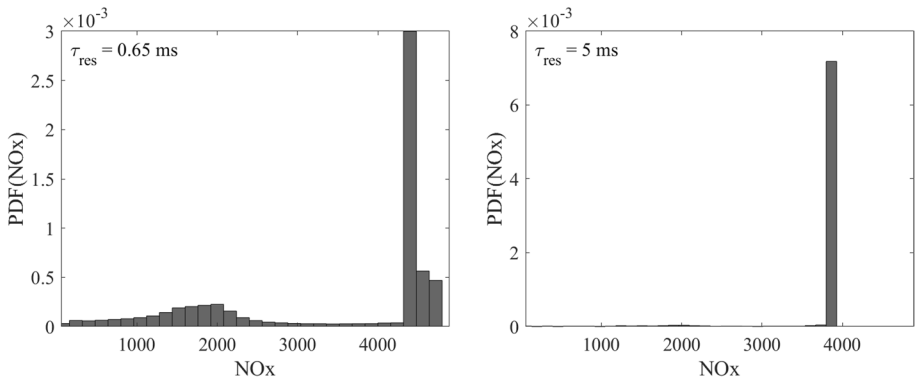

Fig. 10 PDFs of NOx at statistical steady state for two different residence times. Mixing frequency: $\omega_{mix} = 1 \times 10^4$ Hz. Mixture: 70%NH_3–30%H_2-air. Adiabatic system

However, the PDF of the NOx for short residence time (here $\tau_{\text{res}} = 0.65$ ms) deviates from the one for long residence time significantly. For short residence time, the PDF of NOx has two peaks: one with a high peak is similar to the one for long residence time; the other one with a low peak does not exist noticeably for long residence time. This low peak comes from the new incoming cold particles, which are ignited after the mixing process and NOx can be produced from NH_3 only in a small amount due to insufficient reaction time (short residence time). For this case, a combination of two normal distributions must be applied to capture both PDF peaks.

From this short discussion, we can clearly see that although the averaged NOx concentration can be similar for different residence times, statistics (PDFs) can be totally different. This is attributed to its complicated chemical nature, which makes the prediction of NOx in the turbulent case more challenging.

4.3.3 Sensitivity of Chemical Reactions

Since the statistics of the thermo-kinetic states (especially NOx prediction) at long or short residence times can be different, it is of great interest to know whether the residence time will alter important chemical reactions for the NO emission, and whether these important chemical reactions are the same for both PSR and PaSR models. In order to answer such questions, a sensitivity analysis has been performed. The relative sensitivity S^{rel} used in this work describes the normalized sensitivity of NO concentration f_{NO} with respect to the reaction rate of one elementary reaction:

$$\begin{aligned} S^{\text{rel}}_{\text{NO}} &= \frac{k_r}{f_{\text{NO}}} \cdot \frac{\partial f_{\text{NO}}}{\partial k_r} \quad \text{(evaluated by finite difference)} \\ &\approx \frac{k_r}{f_{\text{NO}}} \cdot \frac{\Delta f_{\text{NO}}}{\Delta k_r} = \frac{k_r}{f_{\text{NO}}} \cdot \frac{f_{\text{NO}}(2k_r) - f_{\text{NO}}(k_r)}{2k_r - k_r} = \frac{f_{\text{NO}}(2k_r) - f_{\text{NO}}(k_r)}{f_{\text{NO}}(k_r)}. \end{aligned} \tag{13}$$

Note that we use the brute-force method to evaluate the sensitivity, namely multiplying the k_r with factor 2. The main focus is on the NO species since it is the primary component of NOx. According to the definition of S^{rel}, a positive sensitivity signifies an increase of f_{NO} with increased reaction rate of one elementary reaction, while a negative sensitivity signifies a decrease of f_{NO} with an increased reaction rate. Figure 11 shows the relative sensitivity of NO to reaction rates for PSR and PaSR with two different residence times. The $\tau_{\text{res}} = 0.8$ ms corresponds to the case near extinction, and the $\tau_{\text{res}} = 4.0$ ms corresponds to the case with almost perfect mixing. In this figure, only the elementary reactions with $\text{abs}(S^{\text{rel}}_{\text{NO}}) > 0.01$ are presented. For both residence times, the PSR and PaSR models show the same most sensitive elementary reactions. For all considered models and conditions, the NH+OH=HNO+H shows the largest and most positive sensitivity values. According to reaction pathflow in Chai et al. (2021), the HNO is the main species producing NO species, and the faster this reaction is, the more NO will be produced. The NH+NO=N_2O+H is the second most sensitive reaction, and this reaction is mainly responsible for the consumption of NO, which explains the negative sensitive values.

4.4 Effect of Different Chemical Mechanisms

Since the chemical mechanisms give different results when using the PSR models (c.f. Figure 3), it is necessary to check whether these differences are also observed when using

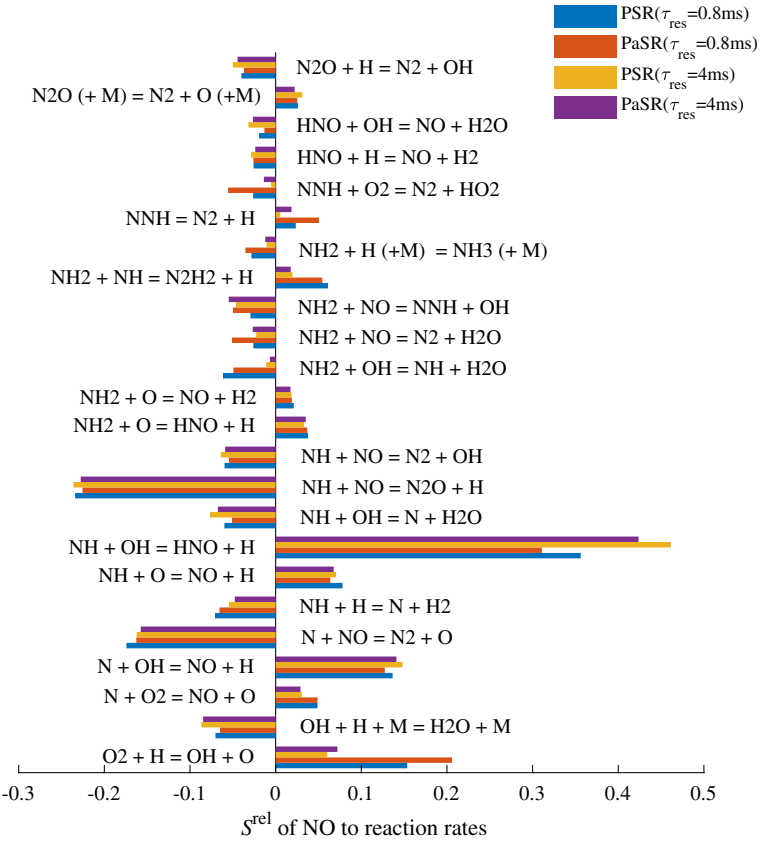

Fig. 11 Relative sensitivity of NO to reaction rates for PSR and PaSR with two different residence time. $\omega_{mix} = 1 \times 10^4$ (Hz). Mixture: 70%NH_3–30%H_2-air. Adiabatic system

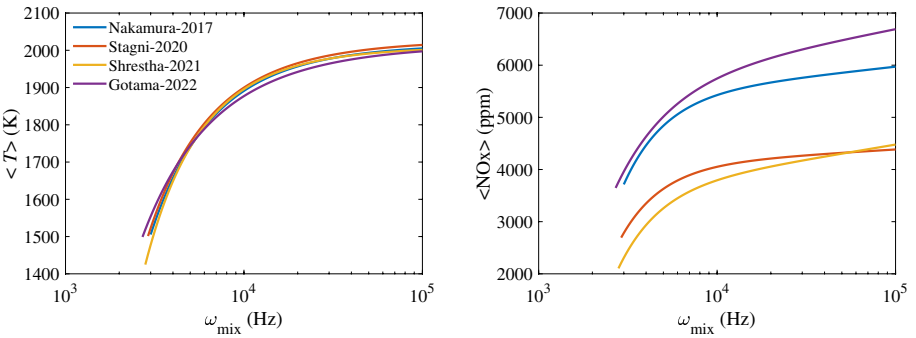

Fig. 12 Influence of mixing frequencies ω_{mix} on the ensemble-averaged temperature $\langle T \rangle$ and NOx emission $\langle$NOx$\rangle$ predicted by four different chemical mechanisms. $\tau_{res} = 1$ ms. Mixture: 70%NH_3+30%H_2+air. Adiabatic system. Blue: Nakamura-2017 (Nakamura et al. 2017); Red: Stagni-2020 (Stagni et al. 2020); Yellow: Shrestha-2021 (Shrestha et al. 2021); Purple: Gotama-2022 (Gotama et al. 2022)

the PaSR model. In order to address this concern, we show in Fig. 12 the influence of mixing frequencies ω_{mix} on the ensemble-averaged temperature $\langle T \rangle$ and NOx emission $\langle$ NOx$\rangle$ predicted by four different chemical mechanisms. In this case, the residence time is kept as $\tau_{\text{res}} = 1$ ms. We notice immediately, as consistent with the observation from Fig. 3, the averaged temperatures predicted by these four different mechanisms are very similar while the averaged NOx can be significantly different. Gotama-2022 (purple lines) shows the highest prediction of NOx while the Stagni-2020 (red lines) and Shrestha-2021 (yellow lines) show similar values, and the NOx predicted by Gotama-2022 can be almost two times larger than predicted by Stagni-2020 and Shrestha-2021.

Although the predicted averaged-NOx can be significantly different by using different chemical mechanisms, Fig. 13 shows that the shapes of the PDF(NOx) are in a similar manner under the same conditions (here $\omega_{\text{mix}} = 5 \times 10^3$ Hz and $\tau_{\text{res}} = 1$ ms). All the PDF(NOx) show two peaks with one low peak in the low NOx concentration regime and the other high peak in the high NOx concentration regime.

In Fig. 14 we show further the sensitivity of NOx with respect to the chemical reaction rate for these four different mechanisms. This figure ensures that 10 most sensitive elementary reactions for each chemical mechanisms are included. Overall these chemical mechanisms show some same reactions such as NH+HO=HNO+H and NH+NO=N_2O+H, which are sensitive to the NO concentration. However, Nakamura-2017 mechanism shows

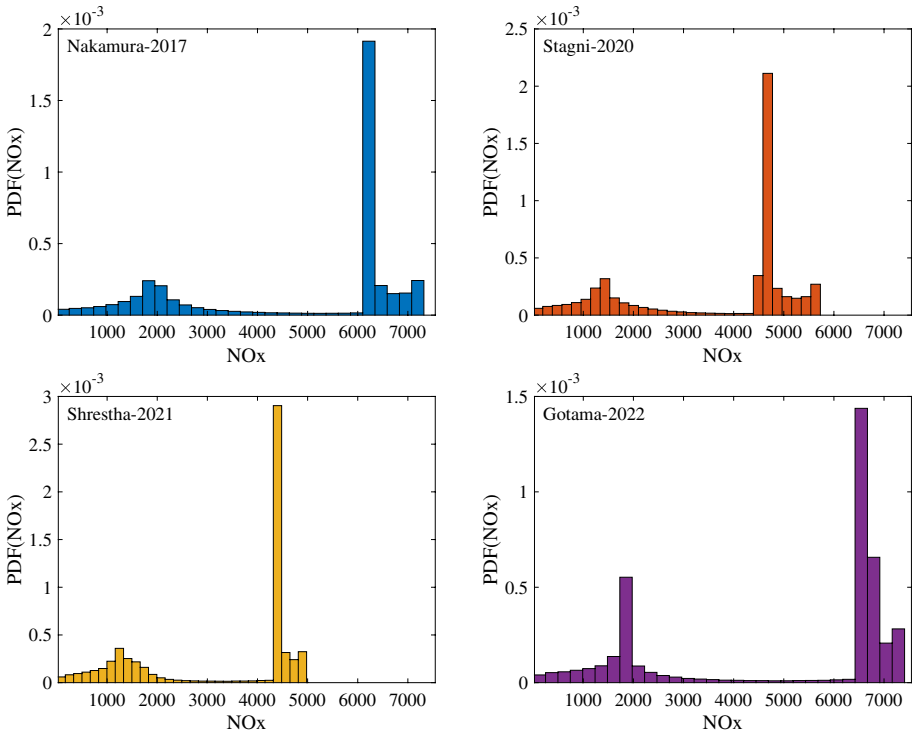

Fig. 13 PDFs of NOx at statistical steady state for four different chemical mechanisms. Mixing frequency: $\omega_{\text{mix}} = 5 \times 10^3$ Hz. Residence time $\tau_{\text{res}} = 1$ ms. Mixture: 70%NH_3–30%H_2-air. Adiabatic system. Blue: Nakamura-2017 (Nakamura et al. 2017); Red: Stagni-2020 (Stagni et al. 2020); Yellow: Shrestha-2021 (Shrestha et al. 2021); Purple: Gotama-2022 (Gotama et al. 2022)

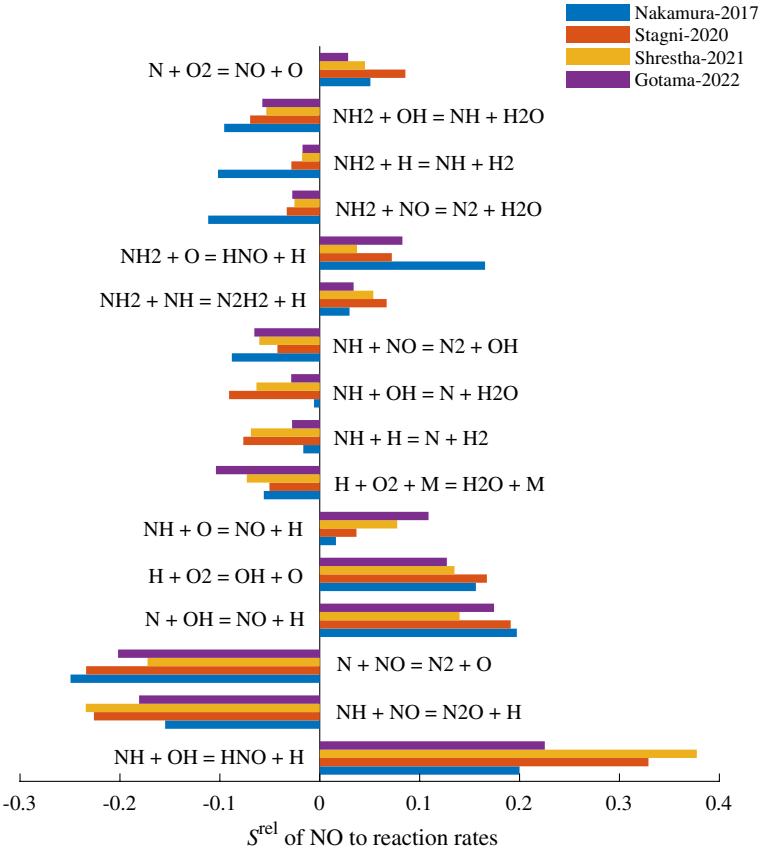

Fig. 14 Relative sensitivity of NO to reaction rates for PaSR with different chemical mechanisms. $\omega_{mix} = 1 \times 10^4$ (Hz), $\tau_{res} = 1$ ms. Mixture: 70%NH_3–30%H_2-air. Adiabatic system. Blue: Nakamura-2017 (Nakamura et al. 2017); Red: Stagni-2020 (Stagni et al. 2020); Yellow: Shrestha-2021 (Shrestha et al. 2021); Purple: Gotama-2022 (Gotama et al. 2022)

that the NH+OH=N+H_2O is not important while the reaction rates of NH_2+NO=N_2+H_2O and NH_2+H=NH+H_2 have large impact on the NO concentration prediction, the other three mechanisms show a weaker impact of these two reactions. Such difference needs to be investigated in more details, if more experimental measurement of NOx concentration is available for the validation of chemical mechanisms.

5 Results: Effect of Hydrogen or Oxygen Enrichment on the PaSR Modeling

So far we focus on the ammonia-air combustion system enriched by 30% hydrogen (70%NH_3–30%H_2-air). As shown in Shrestha et al. (2021), it is found that the 70%NH_3 -30%H_2-air flame and NH_3-30%O_2/70%N_2 flame have similar laminar flame speed. Therefore, it is interesting to see whether both combustion systems have also similar behaviors in the PaSR models, especially the NOx concentration. This section begins with a short

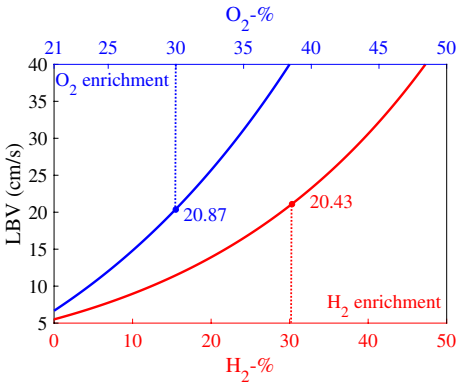

Fig. 15 Comparison of laminar burning velocity (LBV) for the stoichiometric ammonia-air with hydrogen enrichment (red) and with oxygen enrichment (blue). $T_{ub} = 300$ K and $p = 1$ bar. Adiabatic system

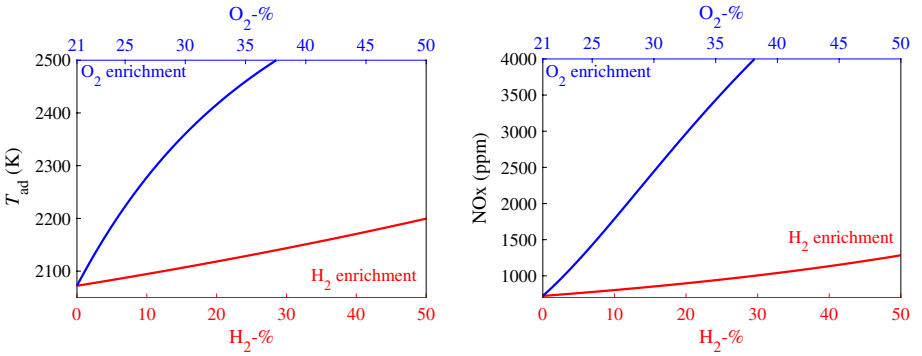

Fig. 16 Comparison of adiabatic flame temperature T_{ad} (left) and NOx emission (right) for the stoichiometric ammonia-air with hydrogen enrichment (red) and with oxygen enrichment (blue). $T_{ub} = 300$ K and $p = 1$ bar

review on the laminar premixed flame for both systems. Then the PaSR prediction of dependence on the mixing frequency will be discussed. The main results of this part are related to the third subsection, where the effect of thermal radiation on the combustion system for both mixtures will be discussed.

5.1 *A-priori* Brief Comparison for Laminar Premixed Flame

Figure 15 shows the comparison of laminar burning velocity (LBV) for the stoichiometric ammonia-air with hydrogen enrichment (red) and with oxygen enrichment (blue). Note that the validation of applied Shrestha-2021 mechanism for ammonia-hydrogen-air and ammonia-oxygen-air in terms of ignition delay times and laminar burning velocity against the experimental measurements can be found in Shrestha et al. (2021). We notice from this figure that both H_2 and O_2 have positive effect on the LBV, which is consistent with those reported in many works such as Mei et al. (2019); Li et al. (2015); Sun et al. (2023); Ichikawa et al. (2015). Furthermore, it is observed that indeed the stoichiometric 70%NH_3–30%H_2-air combustion system and stoichiometric NH_3–30%O_2-70%N_2 combustion system have very similar LBV.

Figure 16 compares further the adiabatic flame temperature T_{ad} (left) and NOx emission (right) for the stoichiometric ammonia-air with hydrogen enrichment (red) and with oxygen enrichment (blue). It is consistent with those shown in Mei et al. (2019); Li et al. (2015); Sun et al. (2023) that the adiabatic flame temperature T_{ad} increases monotonically with increasing H_2 and O_2 contents in the ammonia-air mixtures, and the O_2 has more stronger effect on T_{ad} than the H_2. Desipte the higher T_{ad} due to O_2 enrichment, the corresponding NOx emission of ammonia-air mixture under O_2 enrichment is much higher than it under H_2 enrichment.

5.2 Comparison for PaSR Case

Figure 17 compares the ensemble-averaged temperature $\langle T \rangle$ and NOx emission $\langle \mathrm{NOx} \rangle$ (left y-axis) and their r.m.s. of the fluctuation (right y-axis), if the 70%NH_3–30%H_2-air (red) and NH_3–30%O_2-70%N_2 (blue) mixtures are applied. The major two observations can be addressed here:

- The decrease of mixing frequencies leads to decrease of both $\langle T \rangle$ and $\langle \mathrm{NOx} \rangle$, as explained above. And the extinction mixing frequency $\omega_{\mathrm{mix}}^{\mathrm{E}}$ for both gas mixtures are close to each other. However, as consistent with the observation from Fig. 16, the NH_3 –30%O_2-70%N_2 gas mixture gives higher values of both $\langle T \rangle$ and $\langle \mathrm{NOx} \rangle$. This means that for the consideration of turbulence mixing process, the NH_3–30%O_2-70%N_2 system has higher combustion temperature, but also higher levels of NOx emission.
- The decrease of mixing frequency leads to increase of both r.m.s. of the $\langle T \rangle$ and r.m.s. of the $\langle \mathrm{NOx} \rangle$, as explained above. And their values are similar against the variation of mixing frequency. This indicates that the mixing frequency has the similar effect on the decay of fluctuations for both combustion systems.

5.3 Effect of Thermal Radiation on Both Combustion Systems

In this part, we will focus on the effect of thermal radiation on the studied combustion system. In order to clarify the effect of the thermal radiative heat loss from the combustion

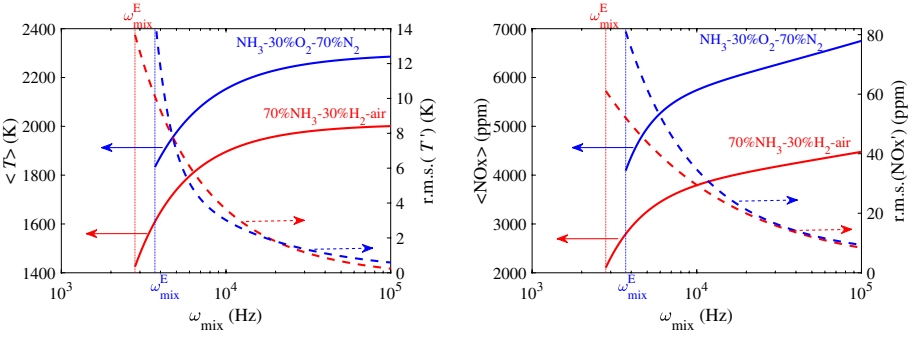

Fig. 17 Influence of mixing frequencies ω_{mix} on the ensemble-averaged temperature $\langle T \rangle$ and NOx emission $\langle \mathrm{NOx} \rangle$ (left y-axis) and their r.m.s. of the fluctuation (right y-axis) for 70%NH_3–30%H_2-air (red) and NH_3 –30%O_2-70%N_2 (blue) mixtures. $\tau_{\mathrm{res}} = 1$ ms. Adiabatic system

system, we introduce the so-called "radiant fraction" f_{rad}, describing the radiative heat loss normalized by the total heat release rate as:

$$f_{\mathrm{rad}} - \% = \frac{\dot{Q}_{\mathrm{rad}}}{\dot{Q}_{\mathrm{HRR}}} \times 100\% = \frac{\dot{Q}_{\mathrm{rad}}}{\sum_{i=1}^{n_s} \dot{\omega}_i h_i} \times 100\%, \tag{14}$$

where $\dot{\omega}_i$ and h_i are the net production rate and enthalpy for species i. Furthermore, we define the Importance of Radiating Species IRS as:

$$\mathrm{IRS}(i) = \frac{\dot{Q}_i^{\mathrm{rad}}}{\dot{Q}_{\mathrm{rad}}} = \frac{\dot{Q}_i^{\mathrm{rad}}}{\sum_{j=1} \dot{Q}_j^{\mathrm{rad}}}, \qquad j : \text{index of radiating species.} \tag{15}$$

For the ammonia-hydrogen-air system, the radiating species are H_2O, NO, N_2O and NH_3 according to Nakamura et al. (2017). And it is shown in Nakamura and Shindo (2019) that the predicted NOx emission by considering the radiative heat loss results in the decrease of NOx emission at high temperature regime and almost no change at low temperature regime (more explanation in Nakamura and Shindo (2019)). For the PaSR, the averaged temperature of the system decreases monotonically with decreasing mixing frequency (see Sect. 4.2). Therefore, it is expected that at low mixing frequency where the averaged temperature is low, the effect of radiation would be small, which is confirmed in Fig. 18(left).

There the time development of averaged temperature and NOx emission under adiabatic and radiative conditions is compared for 70%NH_3–30%H_2-air system under $\omega_{\mathrm{mix}} = 3 \times 10^3$ (Hz) and residence time $\tau_{\mathrm{res}} = 1$ ms over a 6 ms ($6\tau_{\mathrm{res}}$) time interval. Note that for both conditions, the initial conditions are exactly the same. It is observed that the profiles for both adiabatic and radiative conditions develop in almost the same manner, and the effect of thermal radiation at small mixing frequency is not observed. To understand this, we plot in Fig. 18(right) the radiant fraction f_{rad}(right) the radiant fraction f_{rad} and the importance of radiating species (IRS) for all four involved species. We observe that the radiative heat loss is only around 0.02% of the total HRR from 2 ms, which is a very small amount, and this results in a negligibly small influence of thermal radiation on the flame quantities for $\omega_{\mathrm{mix}} = 3 \times 10^3$ (Hz). A further look into the IRS indicates that the H_2O, as a major product, contributes over 95% to the radiative heat loss, then is the NH_3 with around 3% contribution.

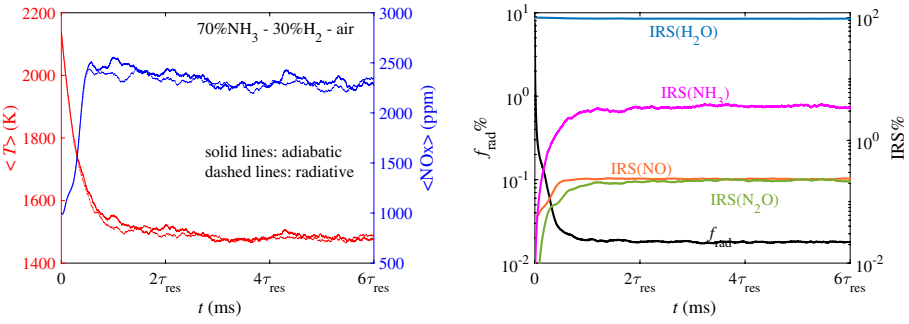

Fig. 18 Comparison of ensemble-averaged temperature $\langle T \rangle$ and NOx emission $\langle \mathrm{NOx} \rangle$ for adiabatic condition (solid lines) and radiative condition (dashed lines) for $\omega_{\mathrm{mix}} = 3 \times 10^3$ (Hz) and residence time $\tau_{\mathrm{res}} = 1$ ms. $T_{\mathrm{ub}} = 300$ K and $p = 1$ bar

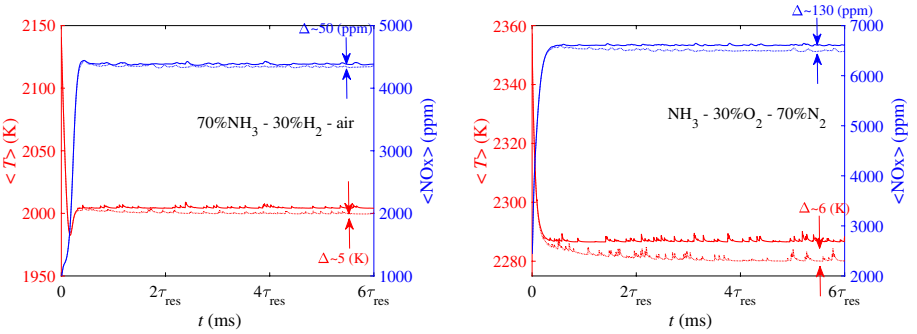

Fig. 19 Comparison of ensemble-averaged temperature $\langle T \rangle$ and NOx emission $\langle \mathrm{NOx} \rangle$ for adiabatic condition (solid lines) and radiative condition (dashed lines) for $\omega_{\mathrm{mix}} = 1 \times 10^5$ (Hz) and residence time $\tau_{\mathrm{res}} = 1$ ms. $T_{\mathrm{ub}} = 300$ K and $p = 1$ bar

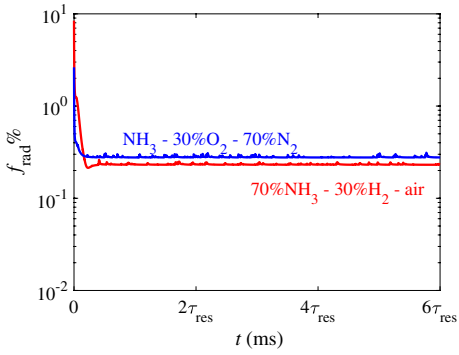

Fig. 20 Comparison of radiant fraction f_{rad} for the stoichiometric ammonia-air with hydrogen enrichment (red) and with oxygen enrichment (blue). $T_{\mathrm{ub}} = 300$ K and $p = 1$ bar

In Fig. 19 comparison of ensemble-averaged temperature $\langle T \rangle$ and NOx emission $\langle \mathrm{NOx} \rangle$ for adiabatic condition (solid lines) and radiative condition (dashed lines) for a larger mixing frequency $\omega_{\mathrm{mix}} = 1 \times 10^5$ (Hz) with residence time $\tau_{\mathrm{res}} = 1$ ms is presented. Again time domain of 6 ms ($6\tau_{\mathrm{res}}$) is shown. We observe that for both mixture compositions, the decrease of temperature caused by thermal radiation is only around 5 K or 6 K, and the decrease of NOx concentration is also small, namely for $70\%NH_3$–$30\%H_2$-air only around 1.5% decrease and for NH_3–$30\%O_2$-$70\%N_2$ only around 2.5% decrease. The radiant fractions for both systems, which are presented in Fig. 20, show that the radiative heat loss is only around 0.2% of the total HRR. These results show that at least for the considered system here, the thermal radiation has only minor effect on the combustion system.

6 Conclusions

In the present work, the Partially Stirred Reactor (PaSR) model is used to investigate the turbulence-chemistry interaction for the ammonia-air combustion system. The PaSR is based on a stochastic modeling by solving the transported PDF equation, and the effect of turbulence mixing is considered by means of the LMSE mixing model. The transprted-PDF method allows us to include the effect of turbulent frequency, and to

investigate the effect of chemical mechanisms since the chemical source term is in a closed form. A comprehensive investigation of different physical and chemical parameters is carried out, and various main observations can be concluded briefly here:

- The effect of the mixing frequency on the ammonia-hydrogen-air system is consistent with those on the hydrocarbon system, namely a decrease in mixing frequency leads to a decrease of thermo-kinetic quantities (e.g. temperature and NOx concentration) and an increase of their fluctuation. The statistics analysis shows that the PDF of the NOx at low turbulent frequency has two peaks while at high turbulent frequency only one. Further analysis shows that the PDFs of different species are closely correlated with each other, and the assumption about statistical independence which is usually used in the presumed PDF method is not valid.
- The effect of residence time on the PaSR model is similar to the one on the PSR model. While the averaged temperature decreases with shorter residence time monotonically, the NOx concentration shows a non-monotonic dependence on the residence time due to the reaction pathway $NH_3 \rightarrow NOx \rightarrow N_2$. Further statistics analysis showed that the shapes of the NOx PDFs can be totally different for different residence times. While the PDF(NOx) at long residence time can be approximated by a $\beta-$function, the PDF(NOx) at short residence time must be approximated by e.g. combining two normal distributions.
- Sensitivity analysis of NOx with respect to the chemical reaction rate displays that the elementary reactions which are sensitive according to the PSR model are also the most sensitive ones according to the PaSR model, independent of residence times.
- Four different chemical mechanisms have been applied and compared for PaSR case, indicating that the predicted NOx can be significantly different. However, the statistics analysis shows that the shapes of PDF(NOx) are in a similar manner by using these four different mechanisms. Further sensitivity analysis of NO with respect to the chemical reaction rates shows that for all these chemical mechanisms the most sensitive reactions such as NH+OH=HNO+H are the same.
- The effect of oxygen enrichment and hydrogen enrichment on the PaSR model prediction is discussed. It is noted that although 30%-O_2 enrichment has a similar effect as 30%-H_2 enrichment in terms of laminar flame speed, the 30%-O_2 enrichment leads to higher averaged temperature and NOx concentration.
- The numerical simulation showed that the thermal radiation gas had little effect on the system, regardless of the mixing frequency.

At the end, it is worth pointing out that all conclusions are obtained and discussed based on the assumption that the mixing frequencies are equal for all thermo-kinetic states. However, various chemical species may have different mixing frequencies due to e.g. the small-scale-turbulence/scalar interactions, which may be of great interest for future research.

Acknowledgements The idea of this paper comes during the preparation of the joint project "Research of combustion reaction kinetics of a multi-component e-fuel for efficient utilization".

Author Contributions Conceptualization: CY; Methodology: CY, LC, JYC; Software and simulations: CY; Validation: CY; Data analysis: CY, LC, JYC; Writing—original draft preparation: CY; Writing—review and editing: CYu, LC, JYC; All authors have reviewed the manuscript.

Funding Open Access funding enabled and organized by Projekt DEAL.

Declarations

Conflict of interest The authors declare that they have no conflict of interest.

References

Abdelwahid, S., Malik, M.R., Hammoud, H.A.A.K., Hernández-Pérez, F.E., Ghanem, B., Im, H.G.: Large eddy simulations of ammonia-hydrogen jet flames at elevated pressure using principal component analysis and deep neural networks. Combust. Flame **253**, 112781 (2023)

Borghi, R.: Turbulent combustion modelling. Prog. Energy Combust. Sci. **14**(4), 245–292 (1988)

Bray, K., Champion, M., Libby, P.A.: The interaction between turbulence and chemistry in premixed turbulent flames, pp. 541–563. In: Turbulent Reactive Flows, Springer, Cham (1989)

Cannon, S., Brewster, B., Smoot, L.: Stochastic modeling of co and no in premixed methane combustion. Combust. Flame **113**(1–2), 135–146 (1998)

Cao, R.R., Wang, H., Pope, S.B.: The effect of mixing models in pdf calculations of piloted jet flames. Proc. Combust. Inst. **31**(1), 1543–1550 (2007)

Celis, C., Silva, L.F.: Lagrangian mixing models for turbulent combustion: review and prospects. Flow Turbul. Combust. **94**, 643–689 (2015)

Chai, W.S., Bao, Y., Jin, P., Tang, G., Zhou, L.: A review on ammonia, ammonia-hydrogen and ammonia-methane fuels. Renew. Sustain. Energy Rev. **147**, 111254 (2021)

Chang, W.-C., Chen, J.-Y.: Impact of mixing model on predicted no formation in a nonpremixed, partially stirred reactor. In: Symposium (International) on Combustion, Vol 26,pp 2223–2229 (1996). Elsevier

Chen, J.-Y.: Stochastic modeling of partially stirred reactors. Combust. Sci. Technol. **122**(1–6), 63–94 (1997)

Chen, Z., Reddy, V., Ruan, S., Doan, N., Roberts, W.L., Swaminathan, N.: Simulation of mild combustion using perfectly stirred reactor model. Proc. Combust. Inst. **36**(3), 4279–4286 (2017)

Chen, J., Jiang, X., Qin, X., Huang, Z.: Effect of hydrogen blending on the high temperature auto-ignition of ammonia at elevated pressure. Fuel **287**, 119563 (2021)

Chiong, M.-C., Chong, C.T., Ng, J.-H., Mashruk, S., Chong, W.W.F., Samiran, N.A., Mong, G.R., Valera-Medina, A.: Advancements of combustion technologies in the ammonia-fuelled engines. Energy Convers. Manage. **244**, 114460 (2021)

Chi, C., Han, W., Thévenin, D.: Effects of molecular diffusion modeling on turbulent premixed nh3/h2/air flames. Proc. Combust. Inst. **39**(2), 2259–2268 (2023)

Cleary, M., Klimenko, A.Y.: A generalised multiple mapping conditioning approach for turbulent combustion. Flow Turbul. Combust. **82**, 477–491 (2009)

Correa, S.M.: Turbulence-chemistry interactions in the intermediate regime of premixed combustion. Combust. Flame **93**(1–2), 41–60 (1993)

Dai, L., Gersen, S., Glarborg, P., Mokhov, A., Levinsky, H.: Autoignition studies of nh3/ch4 mixtures at high pressure. Combust. Flame **218**, 19–26 (2020)

De, A., Oldenhof, E., Sathiah, P., Roekaerts, D.: Numerical simulation of delft-jet-in-hot-coflow (djhc) flames using the eddy dissipation concept model for turbulence-chemistry interaction. Flow Turbul. Combust. **87**, 537–567 (2011)

Dopazo, C., O'Brien, E.E.: An approach to the autoignition of a turbulent mixture. Acta Astronaut. **1**(9–10), 1239–1266 (1974)

Dos Santos, R.G., Ducruix, S., Gicquel, O., Veynate, D.: A study of three-dimensional les of turbulent combustion with radiative heat transfer. J. Braz. Soc. Mech. Sci. Eng. **38**, 33–48 (2016)

Fan, Q., Liu, X., Xu, L., Subash, A.A., Brackmann, C., Aldén, M., Bai, X.-S., Li, Z.: Flame structure and burning velocity of ammonia/air turbulent premixed flames at high karlovitz number conditions. Combust. Flame **238**, 111943 (2022)
Fernández-Tarrazo, E., Gómez-Miguel, R., Sánchez-Sanz, M.: Minimum ignition energy of hydrogen-ammonia blends in air. Fuel **337**, 127128 (2023)
Fox, R.O.: Computational Models for Turbulent Reacting Flows. Cambridge University Press, Cambridge, UK (2003)
Gerlinger, P.: Investigation of an assumed pdf approach for finite-rate chemistry. Combust. Sci. Technol. **175**(5), 841–872 (2003)
Giordano, P., Lentini, D.: Combustion-radiation-turbulence interaction modeling in absorbing/emitting non-premixed flames. Combust. Sci. Technol. **172**(1), 1–22 (2001)
Glarborg, P., Kee, R.J., Grcar, J.F., Miller, J.A.: PSR: A FORTRAN Program for Modeling Well-stirred Reactors, vol. 46. Sandia National Laboratories Livermore, California, USA (1986)
Goodwin, D.G., Moffat, H.K., Schoegl, I., Speth, R.L., Weber, B.W.: Cantera: An Object-oriented Software Toolkit for Chemical Kinetics, Thermodynamics, and Transport Processes. https://www.cantera.org. Version 2.6.0 (2022). https://doi.org/10.5281/zenodo.6387882
Gotama, G.J., Hayakawa, A., Okafor, E.C., Kanoshima, R., Hayashi, M., Kudo, T., Kobayashi, H.: Measurement of the laminar burning velocity and kinetics study of the importance of the hydrogen recovery mechanism of ammonia/hydrogen/air premixed flames. Combust. Flame **236**, 111753 (2022)
Hottel, H., Williams, G., Bonnell, A.: Application of well-stirred reactor theory to the prediction of combustor performance. Combust. Flame **2**(1), 13–34 (1958)
Ichikawa, A., Hayakawa, A., Kitagawa, Y., Somarathne, K.K.A., Kudo, T., Kobayashi, H.: Laminar burning velocity and markstein length of ammonia/hydrogen/air premixed flames at elevated pressures. Int. J. Hydrogen Energy **40**(30), 9570–9578 (2015)
Ichimura, R., Hadi, K., Hashimoto, N., Hayakawa, A., Kobayashi, H., Fujita, O.: Extinction limits of an ammonia/air flame propagating in a turbulent field. Fuel **246**, 178–186 (2019)
Ilbas, M.: The effect of thermal radiation and radiation models on hydrogen-hydrocarbon combustion modelling. Int. J. Hydrogen Energy **30**(10), 1113–1126 (2005)
Landenfeld, T., Sadiki, A., Janicka, J.: A turbulence-chemistry interaction model based on a multivariate presumed beta-pdf method for turbulent flames. Flow Turbul. Combust. **68**, 111–135 (2002)
Lee, S., Kwon, O.C.: Effects of ammonia substitution on extinction limits and structure of counterflow non-premixed hydrogen/air flames. Int. J. Hydrogen Energy **36**(16), 10117–10128 (2011)
Lesmana, H., Zhu, M., Zhang, Z., Gao, J., Wu, J., Zhang, D.: An experimental investigation into the effect of spark gap and duration on minimum ignition energy of partially dissociated nh3 in air. Combust. Flame **241**, 112053 (2022)
Lhuillier, C., Brequigny, P., Contino, F., Mounaïm-Rousselle, C.: Experimental study on ammonia/hydrogen/air combustion in spark ignition engine conditions. Fuel **269**, 117448 (2020)
Li, J., Huang, H., Kobayashi, N., He, Z., Osaka, Y., Zeng, T.: Numerical study on effect of oxygen content in combustion air on ammonia combustion. Energy **93**, 2053–2068 (2015)
Lockwood, F., Naguib, A.: The prediction of the fluctuations in the properties of free, round-jet, turbulent, diffusion flames. Combust. Flame **24**, 109–124 (1975)
Lu, T., Law, C.K.: A directed relation graph method for mechanism reduction. Proc. Combust. Inst. **30**(1), 1333–1341 (2005)
Maas, U., Pope, S.B.: Simplifying chemical kinetics: intrinsic low-dimensional manifolds in composition space. Combust. Flame **88**(3–4), 239–264 (1992)
Marchisio, D.L., Fox, R.O., Barresi, A.A., Baldi, G.: On the comparison between presumed and full pdf methods for turbulent precipitation. Indus. Eng. Chem. Res. **40**(23), 5132–5139 (2001)
Mashruk, S., Kovaleva, M., Alnasif, A., Chong, C.T., Hayakawa, A., Okafor, E.C., Valera-Medina, A.: Nitrogen oxide emissions analyses in ammonia/hydrogen/air premixed swirling flames. Energy **260**, 125183 (2022)
Mashruk, S., Vigueras-Zuniga, M.O., Tejeda-del-Cueto, M.-E., Xiao, H., Yu, C., Maas, U., Valera-Medina, A.: Combustion features of ch4/nh3/h2 ternary blends. Int. J. Hydrogen Energy **47**(70), 30315–30327 (2022)
Mei, B., Zhang, X., Ma, S., Cui, M., Guo, H., Cao, Z., Li, Y.: Experimental and kinetic modeling investigation on the laminar flame propagation of ammonia under oxygen enrichment and elevated pressure conditions. Combust. Flame **210**, 236–246 (2019)
Minamoto, Y., Swaminathan, N.: Subgrid scale modelling for mild combustion. Proc. Combust. Inst. **35**(3), 3529–3536 (2015)
Mukhopadhyay, S., Van Oijen, J., De Goey, L.: A comparative study of presumed pdfs for premixed turbulent combustion modeling based on progress variable and its variance. Fuel **159**, 728–740 (2015)

Nakamura, H., Shindo, M.: Effects of radiation heat loss on laminar premixed ammonia/air flames. Proc. Combust. Inst. **37**(2), 1741–1748 (2019)
Nakamura, H., Hasegawa, S., Tezuka, T.: Kinetic modeling of ammonia/air weak flames in a micro flow reactor with a controlled temperature profile. Combust. Flame **185**, 16–27 (2017)
Poinsot, T., Veynante, D.: Theoretical and Numerical Combustion. RT Edwards Inc., Philadelphia, USA (2005)
Poitou, D., Amaya, J., El Hafi, M., Cuénot, B.: Analysis of the interaction between turbulent combustion and thermal radiation using unsteady coupled les/dom simulations. Combust. Flame **159**(4), 1605–1618 (2012)
Pope, S.B.: Pdf methods for turbulent reactive flows. Prog. Energy Combust. Sci. **11**(2), 119–192 (1985)
Pope, S.B.: A model for turbulent mixing based on shadow-position conditioning. Phys. Fluids **25**(11), 110803 (2013)
Raman, V., Pitsch, H.: A consistent les/filtered-density function formulation for the simulation of turbulent flames with detailed chemistry. Proc. Combust. Inst. **31**(2), 1711–1719 (2007)
Richter, M., Schultheis, R., Dawson, J., Gruber, A., Barlow, R., Dreizler, A., Geyer, D.: Extinction strain rates of premixed ammonia/hydrogen/nitrogen-air counterflow flames. Proc. Combust. Inst. **39**(2), 2027–2035 (2023)
Rocha, R.C., Costa, M., Bai, X.-S.: Chemical kinetic modelling of ammonia/hydrogen/air ignition, premixed flame propagation and no emission. Fuel **246**, 24–33 (2019)
Rocha, R.C., Zhong, S., Xu, L., Bai, X.-S., Costa, M., Cai, X., Kim, H., Brackmann, C., Li, Z., Alden, M.: Structure and laminar flame speed of an ammonia/methane/air premixed flame under varying pressure and equivalence ratio. Energy & Fuels **35**(9), 7179–7192 (2021)
Rutar, T., Horning, D.C., Lee, J.C., Malte, P.C.: Nox dependency on residence time and inlet temperature for lean-premixed combustion in jet-stirred reactors. In: Turbo Expo: Power for Land, Sea, and Air, 78644, 003–06036 (1998). American Society of Mechanical Engineers
Salehi, M., Bushe, W.: Presumed pdf modeling for rans simulation of turbulent premixed flames. Combust. Theor. Model. **14**(3), 381–403 (2010)
Shampine, L.F., Reichelt, M.W.: The matlab ode suite. SIAM J. Sci. Comput. **18**(1), 1–22 (1997)
Shrestha, K.P., Lhuillier, C., Barbosa, A.A., Brequigny, P., Contino, F., Mounaïm-Rousselle, C., Seidel, L., Mauss, F.: An experimental and modeling study of ammonia with enriched oxygen content and ammonia/hydrogen laminar flame speed at elevated pressure and temperature. Proc. Combust. Inst. **38**(2), 2163–2174 (2021)
Shrotriya, P., Wang, P., Jiang, L., Murugesan, M.: Redim-pfdf modelling of turbulent partially-premixed flame with inhomogeneous inlets using top-hat function for multi-stream mixing problem. Aerosp. Sci. Technol. **107**, 106258 (2020)
Singh, A.S., Dash, S.K., Reddy, V.M.: Chemical kinetic analysis on influence of hydrogen enrichment on the combustion characteristics of ammonia air using newly proposed reaction model. Int. J. Energy Res. **46**(5), 6144–6163 (2022)
Stagni, A., Cavallotti, C., Arunthanayothin, S., Song, Y., Herbinet, O., Battin-Leclerc, F., Faravelli, T.: An experimental, theoretical and kinetic-modeling study of the gas-phase oxidation of ammonia. React. Chem. Eng. **5**(4), 696–711 (2020)
Subramaniam, S., Pope, S.B.: A mixing model for turbulent reactive flows based on euclidean minimum spanning trees. Combust. Flame **115**(4), 487–514 (1998)
Sun, Z., Huang, Y., Luan, Z., Gao, S., You, Y.: Three-dimensional simulation of a rotating detonation engine in ammonia/hydrogen mixtures and oxygen-enriched air. Int. J. Hydrogen Energy **48**(12), 4891–4905 (2023)
Tian, T., Song, C., Wang, H., Xu, C., Luo, K., Fan, J.: The effects of turbulence on the flame structure and no formation of ammonia turbulent premixed combustion at various equivalence ratios. Fuel **332**, 126127 (2023)
Turns, S.R., et al.: Introduction to Combustion, vol. 287. McGraw-Hill Companies, New York, NY, USA (1996)
Valera-Medina, A., Xiao, H., Owen-Jones, M., David, W.I., Bowen, P.: Ammonia for power. Prog. Energy Combust. Sci. **69**, 63–102 (2018)
Valera-Medina, A., Gutesa, M., Xiao, H., Pugh, D., Giles, A., Goktepe, B., Marsh, R., Bowen, P.: Premixed ammonia/hydrogen swirl combustion under rich fuel conditions for gas turbines operation. Int. J. Hydrogen Energy **44**(16), 8615–8626 (2019)
Valera-Medina, A., Amer-Hatem, F., Azad, A., Dedoussi, I., De Joannon, M., Fernandes, R., Glarborg, P., Hashemi, H., He, X., Mashruk, S., et al.: Review on ammonia as a potential fuel: from synthesis to economics. Energy & Fuels **35**(9), 6964–7029 (2021)

Wang, P., Fröhlich, J., Maas, U., He, Z.-x, Wang, C.-j: A detailed comparison of two sub-grid scale combustion models via large eddy simulation of the preccinsta gas turbine model combustor. Combust. Flame **164**, 329–345 (2016)

Wang, S., Elbaz, A.M., Wang, Z., Roberts, W.L.: The effect of oxygen content on the turbulent flame speed of ammonia/oxygen/nitrogen expanding flames under elevated pressures. Combust. Flame **232**, 111521 (2021)

Xiao, H., Valera-Medina, A., Bowen, P.J.: Modeling combustion of ammonia/hydrogen fuel blends under gas turbine conditions. Energy & Fuels **31**(8), 8631–8642 (2017)

Xu, J., Huang, D., Chen, R., Meng, H.: An improved no prediction model for large eddy simulation of turbulent combustion. Flow Turbul. Combust. **106**, 881–899 (2021)

Yu, C.: Matlab-based *PaSR-PDF* code. https://github.com/ChunkanYu/Stochastic-Modeling-PaSR-for-Combustion (2023)

Yu, C., Eckart, S., Essmann, S., Markus, D., Valera-Medina, A., Schießl, R., Shu, B., Krause, H., Maas, U.: Investigation of spark ignition processes of laminar strained premixed stoichiometric nh3-h2-air flames. J. Loss Prev. Process Ind. **83**, 105043 (2023)

Zheng, S., Liu, H., Wang, Y., Chen, X., Sui, R., Lu, Q.: On the roles of humidification and radiation during the ignition of ammonia-hydrogen-air mixtures. Combust. Flame **254**, 112832 (2023)